

Application of the Wave Based Method for the calculation of structural intensity and power flow in plates

K. Vergote, D. Vandepitte, W. Desmet

K.U.Leuven, Department of Mechanical Engineering,
Celestijnenlaan 300 B - box 2420, B-3001, Heverlee, Belgium
e-mail: karel.vergote@mech.kuleuven.be

Abstract

The Wave Based Method (WBM) is a deterministic prediction method. Due to its enhanced computational efficiency as compared to other deterministic prediction techniques for steady-state dynamic analysis such as the Finite Element Method (FEM), the WBM is applicable for problem analysis in the low- and mid-frequency range.

It has been shown already that the WBM is superior to the FEM for the prediction of dynamic displacement fields. This paper discusses application of the WBM for the computation of structural intensity and power flow in Kirchhoff plates. Such calculations require higher-order derivatives of the displacement fields which even further narrows the low-frequency application range of conventional element based methods such as the FEM because of the low-order polynomial field approximations. The WBM adopts wave-like functions instead of low-order polynomials and, as such, is expected to yield faster and more accurate intensity predictions.

1 Introduction

Due to the ever more restrictive legal regulations and the increased customer comfort expectations, the vibrational and acoustical behaviour of a product has become an important criterion in the product design process. In order to restrict the use of expensive and time-consuming physical prototypes to a minimum, virtual prototypes gained in importance over the last years. In order to develop virtual prototypes, efficient and accurate numerical prediction techniques are required. Since the vibro-acoustic behaviour of a product is often predominantly determined by the behaviour of the involved mechanical structures, this paper focusses on the numerical prediction of that behaviour.

An interest in the calculation of structural intensity arises from the fact that the energy flow distribution gives insight in the energy transmission paths and positions of sources and sinks of mechanical energy. The effect of adding dissipative elements, modifying the mechanical structure or active vibration control can be studied. Experimental methods [1, 2, 3] can be used to determine the structural intensity. However, as mentioned above, the efficient numerical prediction techniques are indispensable. Currently, there are two groups of numerical prediction techniques, i.e. the deterministic and the probabilistic.

From the group of deterministic prediction techniques, the Finite Element Method (FEM) [4] is most commonly used. The FEM discretises the problem domain into a large number of small elements in which the dynamic field variables are approximated by simple polynomial shape functions. As the spatial variation of the dynamic response increases with frequency, the number of elements needed to accurately describe the dynamic response increases. This results in an exponentially increasing computational load when frequency increases, limiting the practical application of the FEM to problems in the low-frequency range. The FEM has been used to determine structural intensity and power flow [5, 6]. However, in order to calculate structural intensity, third-order derivatives are required. These derivatives are calculated using the element shape

functions, which are polynomials. As a result each step of derivation leads to a loss of accuracy.

Among the probabilistic techniques, the methods based on Statistical Energy Analysis (SEA) [7] are mostly used. SEA methods divide the system in a limited number of subsystems, for which frequency- and space-averaged energy levels are predicted. These methods are much less computationally expensive, but are only applicable if all subsystems exhibit, amongst others, a high modal overlap, which limits their use to high-frequency applications.

For mid-frequency applications, currently no efficient and mature prediction techniques exist. Recently a new deterministic technique, called the Wave Based Method (WBM), has been developed [8], which has shown to be able to successfully tackle structural dynamic problems in the mid-frequency range [9, 10, 11]. The method is based on an indirect Trefftz approach [12] in that the dynamic response variables are described in terms of wave functions which exactly satisfy the governing differential equations. In that way, no approximation error is made inside the problem domain. However, the wave functions may violate the boundary and continuity conditions. Therefore, the approximation errors on the domain boundaries and interfaces are minimized by means of a weighted residual formulation. This approach leads to substantially smaller system matrices as compared to the FEM, which results in an enhanced computational efficiency. As a result, the WBM is able to not only tackle applications in the low-frequency range, but also in the mid-frequency range. Since the used basis functions are analytical expressions which satisfy the governing differential equations, it is expected that derived quantities, and thus the structural intensity, will suffer less from loss of accuracy compared to the FEM.

The paper starts with the description of the plate bending problem and the definition of structural intensity. The following section describes the principles of the WBM, the use of springs and dampers in the WBM and how to determine structural intensity. A numerical example demonstrates the validity and the efficiency of the presented method.

2 Mathematical problem description

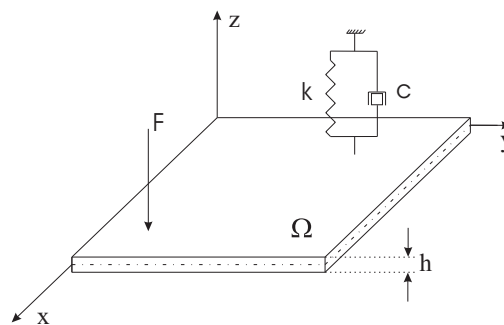


Figure 1: A flat plate excited by a point force F and with a spring k and damper c .

This paper focuses on the intensity calculation for flat plates, excited by a point force normal to the plate. The point force adds energy to the system and a one-dimensional damper, normal to the plate, is added as an energy sink.

Assuming that the plate has symmetric material properties with respect to the middle plane, that sections normal to the middle plane remain plane during deformation and that the direct stresses normal to the plate are small, the in-plane (“membrane”) displacements and the out-of-plane (“bending”) displacements can be considered as decoupled. Since only normal external forces act on the plate, it is sufficient to look at the bending behaviour.

Two important plate bending theories exist, namely the Kirchhoff theory [13] and the Reissner-Mindlin theory [14, 15]. For thin plates, it is shown that the Kirchhoff theory yields accurate results [16].

According to the Kirchhoff theory, the steady-state out-of-plane displacements w_z are governed by the following fourth-order partial differential equation,

$$\nabla^4 w_z(x, y) - k_b^4 w_z(x, y) = \frac{F_z}{D} \delta(x_F, y_F), \tag{1}$$

where $\nabla^4 = \frac{\partial^4}{\partial x^4} + 2\frac{\partial^4}{\partial x^2 \partial y^2} + \frac{\partial^4}{\partial y^4}$. The plate bending wave number k_b and plate bending stiffness D are defined as,

$$k_b = \sqrt[4]{\frac{\rho h \omega^2}{D}}, \tag{2}$$

$$D = \frac{E(1 + j\eta)h^3}{12(1 - \nu^2)}, \tag{3}$$

with h, E, ν, η and ρ respectively the plate thickness, the elasticity modulus, the Poisson coefficient, the material loss factor and the density, and $j = \sqrt{-1}$. The plate is excited with a normal point force F in point (x_F, y_F) .

Since the Kirchhoff theory is governed by a fourth-order partial differential equation, two boundary conditions need to be imposed at the plate boundary Γ . In case of simply supported edges, the out-of-plane displacement and the bending moment are prescribed,

$$\begin{cases} R_{w_z} = w_z - \bar{w}_z = 0 \\ R_{m_n} = \mathcal{L}_{m_n}[w_z] - \bar{m}_n = 0 \end{cases} \tag{4}$$

with \bar{w}_z and \bar{m}_n the prescribed values for the transverse displacement and the bending moment, here both zero, and \mathcal{L}_{m_n} the differential operator for the bending moment, defined as:

$$\mathcal{L}_{m_n} = -D \left(\frac{\partial^2}{\partial n^2} + \nu \frac{\partial^2}{\partial s^2} \right), \tag{5}$$

with n the in-plane normal direction of the plate boundary Γ of the domain. The reader is referred to [9] for the boundary conditions for clamped and free edges.

The instantaneous structural intensity $i_k(t)$ is a time dependent vectorial quantity equal to the change of energy density in a given infinitesimal volume [5]. Its k th component is defined by the relationship

$$i_k(t) = -\sigma_{kl}(t)v_l(t), \quad k = x, y, z \text{ and } l = x, y, z, \tag{6}$$

with $\sigma_{kl}(t)$ the kl th component of the stress tensor and $v_l(t)$ the l th component of the velocity vector. The equation is written in the Einstein Sum Convention. Integration over one period and over the plate thickness leads to [6]:

$$I_x = -\frac{1}{2} \text{Re} \left[Q_x v_z^* - M_x \dot{\theta}_y^* + M_{xy} \dot{\theta}_x^* + F_x v_x^* + F_{xy} v_y^* \right], \tag{7}$$

$$I_y = -\frac{1}{2} \text{Re} \left[Q_y v_z^* + M_y \dot{\theta}_x^* - M_{yx} \dot{\theta}_y^* + F_y v_y^* + F_{yx} v_x^* \right], \tag{8}$$

with:

Q_x, Q_y = transverse shear forces,

M_x, M_y = bending moments,

M_{xy}, M_{yx} = twisting moment about x and y,

F_x, F_y = membrane forces,

F_{xy}, F_{yx} = membrane shear forces,

$v_k, \dot{\theta}_k$ = local translational velocities in direction k and rotational velocities about axis k ,

and * indicating the complex conjugate.

In the case of pure Kirchhoff bending the intensity expressions (7)-(8) can be simplified to:

$$I_x = -\frac{1}{2} \text{Re} \left[Q_x v_z^* - M_x \dot{\theta}_y^* \right], \quad (9)$$

$$I_y = -\frac{1}{2} \text{Re} \left[Q_y v_z^* + M_y \dot{\theta}_x^* \right], \quad (10)$$

with [17],

$$Q_x = -D \frac{\partial}{\partial x} \left(\frac{\partial^2 w_z}{\partial x^2} + (2 - \nu) \frac{\partial^2 w_z}{\partial y^2} \right), \quad (11)$$

$$Q_y = -D \frac{\partial}{\partial y} \left(\frac{\partial^2 w_z}{\partial y^2} + (2 - \nu) \frac{\partial^2 w_z}{\partial x^2} \right), \quad (12)$$

$$M_x = -D \left(\frac{\partial^2 w_z}{\partial x^2} + \nu \frac{\partial^2 w_z}{\partial y^2} \right), \quad (13)$$

$$M_y = -D \left(\frac{\partial^2 w_z}{\partial y^2} + \nu \frac{\partial^2 w_z}{\partial x^2} \right). \quad (14)$$

3 Wave Based Method

The WBM belongs to the category of indirect Trefftz methods [12]. The WBM partitions the problem domain into a small number of subdomains. According to the Trefftz principle, the field variables within each subdomain are approximated by an expansion of basis functions, which exactly satisfy the governing dynamic equations. In this way, there is only an approximation error introduced in the boundary conditions and in the conformity between the subdomains. These errors are forced to zero in an integral sense through the application of a Galerkin-like weighted residual formulation.

The introduction of a spring-damper combination in the WBM can be dealt with similarly to the introduction of point masses described in [18], which adds a particular solution to the field variable expansion.

Once the displacement field can be determined, the structural intensity can be calculated as a postprocessing process.

3.1 Field variable expansion

The steady-state out-of-plane displacement w_z is approximated by the following field variable expansion,

$$w_z(\mathbf{x}) \approx \hat{w}_z(\mathbf{x}) = \sum_{b=1}^{n_b} w_b \Psi_b(\mathbf{x}) + \hat{w}_F(\mathbf{x}) = \mathbf{\Psi}(\mathbf{x}) \cdot \mathbf{w} + \hat{w}_F(\mathbf{x}), \quad (15)$$

with $\Psi_b(\mathbf{x})$ and w_b the wave functions and the corresponding contribution factors, respectively, and $\mathbf{\Psi}(\mathbf{x})$ and \mathbf{w} vectors containing those wave functions and contribution factors. The particular solution $\hat{w}_F(\mathbf{x})$ satisfies the inhomogeneous part of equation (1), arising from an external loading. The displacement field of an infinite plate excited with a normal point force [19] is selected as particular solution,

$$\hat{w}_F = -\frac{jF}{8k_b^2 D} \left[H_0^{(2)}(k_b r_F) - H_0^{(2)}(-jk_b r_F) \right], \quad (16)$$

with $r_F = \sqrt{(x - x_F)^2 + (y - y_F)^2}$.

Each wave function Ψ_b should satisfy the homogeneous part of the dynamic plate bending equation (1). VANMAELE ET AL. [9] propose the wave functions listed in Table 1. These wave functions are divided into two sets. For the first set of wave functions, the functions associated with the first wavenumber are cosine functions. For the second set, the functions associated with the first wavenumber are sine functions. It has been proven by DESMET [8] that the first set of wave functions is theoretically sufficient for the convergence of the WBM, provided that the domain is convex. In practice however, it is shown that at least a few functions of the second set are required for a beneficial convergence rate [17].

	Bending wave functions	
set 1	$\Psi_{b_1}(\mathbf{x}) = \cos(k_{b_1,x}x) \exp(-jk_{b_1,y}y)$	$b_1 = 0, 1, \dots, n_{b_1}$
	$\Psi_{b_2}(\mathbf{x}) = \exp(-jk_{b_2,x}x) \cos(k_{b_2,y}y)$	$b_2 = 0, 1, \dots, n_{b_2}$
set 2	$\Psi_{b_1}(\mathbf{x}) = \sin(k_{b_1,x}x) \exp(-jk_{b_1,y}y)$	$b_1 = 1, \dots, n'_{b_1}$
	$\Psi_{b_2}(\mathbf{x}) = \exp(-jk_{b_2,x}x) \sin(k_{b_2,y}y)$	$b_2 = 1, \dots, n'_{b_2}$

Table 1: Sets of wave functions for plate bending.

An infinite number of wave functions satisfy the homogeneous differential equations. A truncated set must be selected for each field variable. The selection is based on the dimensions ($L_x \times L_y$) of the preferably smallest rectangular box circumscribing the problem domain. DESMET [8] chooses the first wavenumber such that an integer number of half wavelengths equals the dimension of the rectangular box in the corresponding direction,

$$k_{xb_1} = \frac{b_1\pi}{L_x} \quad \text{and} \quad k_{yb_2} = \frac{b_2\pi}{L_y}, \tag{17}$$

with $(b_1, b_2) = 0, \pm 1, \dots$. The other component of the wavenumber is calculated from the structural bending wavenumber k_b corresponding to the considered frequency,

$$k_{yb_1} = \begin{cases} \pm \sqrt{k_b^2 - k_{xb_1}^2} \\ \pm j \sqrt{k_b^2 + k_{xb_1}^2} \end{cases} \quad \text{and} \quad k_{xb_2} = \begin{cases} \pm \sqrt{k_b^2 - k_{yb_2}^2} \\ \pm j \sqrt{k_b^2 + k_{yb_2}^2} \end{cases}. \tag{18}$$

The number of bending wave functions n_b that are included in the field variable expansion (15), is related to the frequency and the dimensions of the enclosing bounding box,

$$n_b = 4(n_{b_1} + 1) + 4(n_{b_2} + 1) + 4n'_{b_1} + 4n'_{b_2}, \tag{19}$$

with,

$$\frac{n_{b_1}}{L_x} \approx \frac{n_{b_2}}{L_y} \approx \frac{n'_{b_1}}{L_x} \approx \frac{n'_{b_2}}{L_y} \geq T \frac{k_b}{\pi}, \tag{20}$$

with $n_{b_1}, n_{b_2}, n'_{b_1}$ and n'_{b_2} integer truncation values and with T a user defined truncation parameter. In this way the largest wave number included in the model is T times the structural wavenumber at this frequency.

3.2 Evaluation of boundary conditions

The wave functions proposed in Table 1 satisfy the governing partial differential equation (1). The boundary conditions are enforced through a weighted residual formulation. The residuals on the boundary conditions (4) are orthogonalized with respect to a weighting function \tilde{w}_z or its derivative. In the case that all boundaries are simply supported, the weighted residual formulation is expressed as,

$$\int_{\Gamma} \mathcal{L}_{Q_n} [\tilde{w}_z] R_{w_z} d\Gamma + \int_{\Gamma} \mathcal{L}_{\theta_n} [\tilde{w}_z] R_{m_n} d\Gamma = 0, \quad (21)$$

with \mathcal{L}_{Q_n} and \mathcal{L}_{θ_n} the differential operation for the generalised shear force and the normal rotation defined as follows,

$$\mathcal{L}_{Q_n} = -D \frac{\partial}{\partial n} \left(\frac{\partial^2}{\partial n^2} + (2 - \nu) \frac{\partial^2}{\partial s^2} \right), \quad (22)$$

$$\mathcal{L}_{\theta_n} = -\frac{\partial}{\partial n}. \quad (23)$$

Like in the Galerkin weighting procedure, used in the FEM, the weighting functions \tilde{w}_z are expanded in terms of the same set of wave functions used in the field variable expansion (15):

$$\tilde{w}_z = \sum_{b=1}^{n_b} \tilde{w}_b \Psi_b(\mathbf{x}) = \mathbf{\Psi}(\mathbf{x}) \cdot \tilde{\mathbf{w}}. \quad (24)$$

Substitution of the field variable expansion (15) and the weighting function expansion (24) into the weighted residual formulation (21) yields:

$$\tilde{\mathbf{w}}^T [\mathbf{A} \cdot \mathbf{w} - \mathbf{f}] = 0. \quad (25)$$

Since weighted residual formulation (21) should hold for any weighting function \tilde{w}_z , the expression between the square brackets in equation (25) must be zero. This yields a matrix equation consisting of n_b algebraic equations in the n_b unknown wave function contribution factors:

$$[\mathbf{A}] \{\mathbf{w}\} = \{\mathbf{b}\} \quad (26)$$

As for the Boundary Element Method (BEM) and in contrast with the FEM, the WBM yields a fully populated matrix, whose elements are complex and which cannot be decomposed into frequency independent submatrices. The big advantage of the WBM is, however, that the system matrices are substantially smaller in comparison with the element based techniques. This property, combined with the fast convergence of the WBM, makes it a less computationally demanding method for dynamic response calculations, which creates opportunities to tackle problems also in the mid-frequency range.

3.3 Local spring and damper

In order to introduce a local spring and damper into the WBM formulation, a particular solution \hat{w}_d , similar to the particular solution of a point force (16), can be added to the field variable expansion (15):

$$w_z(\mathbf{x}) \approx \hat{w}_z(\mathbf{x}) = \sum_{b=1}^{n_b} w_b \Psi_b(\mathbf{x}) + \hat{w}_F(\mathbf{x}) + \hat{w}_d(\mathbf{x}), \quad (27)$$

This approach is similar to the approach for introducing a point mass, described in [18].

The force exerted by a local spring and damper with a stiffness k_d and a damping rate c_d is given by:

$$F = -k_d \Delta l - c_d v, \tag{28}$$

with Δl the spring deformation and v the velocity. Since we are looking at steady-state dynamics, the former expression can be rewritten as:

$$F = F_d e^{j\omega t} = - (k_d + j\omega c_d) W_d e^{j\omega t}, \tag{29}$$

and thus,

$$F_d = - (k_d + j\omega c_d) W_d, \tag{30}$$

with F_d and W_d the amplitudes of respectively the spring-damper force and the displacement of the spring-damper, ω the circular frequency and t the time.

Using (30) in the particular solution of a point force (16), the particular solution for a spring-damper combination \hat{w}_d becomes:

$$\hat{w}_d = \frac{j(k_d + j\omega c_d) W_d}{8k_b^2 D} \left[H_0^{(2)}(k_b r_d) - H_0^{(2)}(-jk_b r_d) \right], \tag{31}$$

with $r_d = \sqrt{(x - x_d)^2 + (y - y_d)^2}$ and (x_d, y_d) the position of the spring-damper combination.

Introducing the expression (27) into the weighted residual formulation (21) with the same weighting functions (24), leads to the following matrix equation,

$$\{\tilde{\mathbf{w}}\}^T \left[\begin{bmatrix} \mathbf{A} & \mathbf{A}' \end{bmatrix} \begin{Bmatrix} \mathbf{w} \\ W_d \end{Bmatrix} - \{\mathbf{f}\} \right] = 0, \tag{32}$$

with,

$$\begin{aligned} \mathbf{A}' = & \int_{\Gamma} \mathcal{L}_{Q_n}(\Psi^T(\mathbf{x})) \frac{j(k_d + j\omega c_d)}{8k_b^2 D} \left[H_0^{(2)}(k_b r_d) - H_0^{(2)}(-jk_b r_d) \right] d\Gamma \\ & + \int_{\Gamma} \mathcal{L}_{\theta_n}(\Psi^T(\mathbf{x})) \mathcal{L}_{m_n} \left(\frac{j(k_d + j\omega c_d)}{8k_b^2 D} \left[H_0^{(2)}(k_b r_d) - H_0^{(2)}(-jk_b r_d) \right] \right) d\Gamma. \end{aligned} \tag{33}$$

Since the system equation (32) contains one unknown (W_d) more than it contains equations, an extra equation is needed. The displacement W_d is equal to the evaluation of the field variable expansion (27) at the position of the spring-damper combination, which, in its turn, can be expressed in function of the unknowns w_b ($b = 1 \dots n_b$) and W_d ,

$$W_d = \sum_{b=1}^{n_b} w_b \Psi_b(\mathbf{x}_d) + \hat{w}_F(\mathbf{x}_d) + \hat{w}_d(\mathbf{x}_d). \tag{34}$$

Using this displacement continuity equation as additional equation for the system (32) leads to a solvable system with unknowns w_b ($b = 1 \dots n_b$) and W_d , which is illustrated in figure 2.

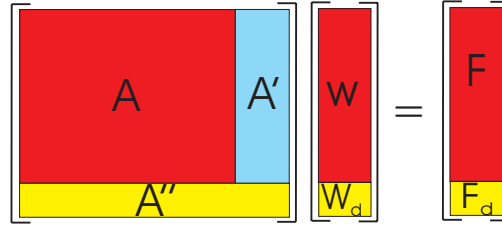


Figure 2: Visualisation of the system matrix equation.

3.4 Structural intensity

To calculate the structural intensity (9)-(10), the shear forces (11)-(12) and bending moments (13)-(14) are required. Substituting the field variable expansion (27) leads to:

$$Q_x = -D \left(\sum_{b=1}^{n_b} w_b \frac{\partial^3 \Psi_b}{\partial x^3} + \frac{\partial^3 \hat{w}_F}{\partial x^3} + \frac{\partial^3 \hat{w}_d}{\partial x^3} - (2 - \nu) \left(\sum_{b=1}^{n_b} w_b \frac{\partial^3 \Psi_b}{\partial x \partial y^2} + \frac{\partial^3 \hat{w}_F}{\partial x \partial y^2} + \frac{\partial \hat{w}_d}{\partial x \partial y^2} \right) \right), \quad (35)$$

$$Q_y = -D \left(\sum_{b=1}^{n_b} w_b \frac{\partial^3 \Psi_b}{\partial y^3} + \frac{\partial^3 \hat{w}_F}{\partial y^3} + \frac{\partial^3 \hat{w}_d}{\partial y^3} - (2 - \nu) \left(\sum_{b=1}^{n_b} w_b \frac{\partial^3 \Psi_b}{\partial x^2 \partial y} + \frac{\partial^3 \hat{w}_F}{\partial x^2 \partial y} + \frac{\partial \hat{w}_d}{\partial x^2 \partial y} \right) \right), \quad (36)$$

$$M_x = -D \left(\sum_{b=1}^{n_b} w_b \frac{\partial^2 \Psi_b}{\partial x^2} + \frac{\partial^2 \hat{w}_F}{\partial x^2} + \frac{\partial^2 \hat{w}_d}{\partial x^2} + \nu \left(\sum_{b=1}^{n_b} w_b \frac{\partial^2 \Psi_b}{\partial y^2} + \frac{\partial^2 \hat{w}_F}{\partial y^2} + \frac{\partial^2 \hat{w}_d}{\partial y^2} \right) \right), \quad (37)$$

$$M_y = -D \left(\sum_{b=1}^{n_b} w_b \frac{\partial^2 \Psi_b}{\partial y^2} + \frac{\partial^2 \hat{w}_F}{\partial y^2} + \frac{\partial^2 \hat{w}_d}{\partial y^2} + \nu \left(\sum_{b=1}^{n_b} w_b \frac{\partial^2 \Psi_b}{\partial x^2} + \frac{\partial^2 \hat{w}_F}{\partial x^2} + \frac{\partial^2 \hat{w}_d}{\partial x^2} \right) \right). \quad (38)$$

These equations only depend on the position on the plate and the calculated contribution factors w_b and the displacement W_d . All the derivatives can be determined easily analytically. As a result, the intensity calculations can be made without loss of accuracy.

4 Numerical example

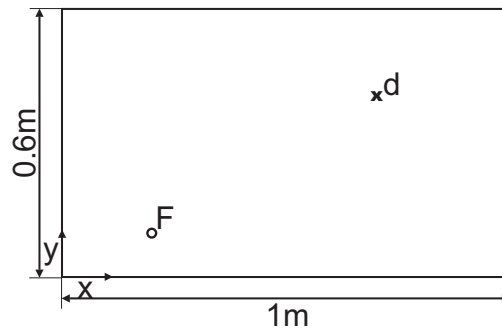


Figure 3: Problem geometry.

In order to validate the described methodology and to show its capabilities a numerical example is given. The considered problem geometry is shown in figure 3. A rectangular geometry has been chosen since an analytical solution is available for that case. The problem consists of a simply supported steel plate, with thickness $h = 1.5\text{mm}$, Young's modulus $E = 210 \cdot 10^9\text{N/m}^2$, Poisson coefficient $\nu = 0.3$, damping loss factor $\eta = 0$ and density $\rho = 7850\text{kg/m}^3$. A unit point force is applied at $F(0.2\text{m}, 0.1\text{m})$. A one-dimensional damper with damping rate $c_d = 100\text{Ns/m}$ is located at $d(0.7\text{m}, 0.4\text{m})$.

First, an analytical solution based on modal superposition with analytically determined mode numbers and mode shapes is defined. Secondly contour plots of the displacement and the structural intensity calculated with the WBM are compared with the analytical solution. Finally some convergence curves demonstrate the quick convergence of the method.

All calculations were performed in MATLAB R2007b on a Intel Centrino Core 2 Duo of 2.2 GHz, with 2 GB RAM running Windows Vista.

4.1 Analytical solution

Since the plate is rectangular, one can derive its modes analytically. Using modal superposition, one can achieve an analytical solution [5]. However the exact solution will only be achieved for an infinite series.

The natural frequencies ω_{nm} and mode shapes Φ_{nm} for a simply supported plate are given by [5]:

$$\omega_{nm}^2 = \frac{DL_xL_y}{M} \left(\frac{n^2\pi^2}{L_x^2} + \frac{m^2\pi^2}{L_y^2} \right)^2, \quad (39)$$

$$\Phi_{nm}(x, y) = 2 \sin\left(\frac{n\pi x}{L_x}\right) \sin\left(\frac{m\pi y}{L_y}\right), \quad (40)$$

with L_x and L_y the dimensions of the plate, M the total mass and $D = \frac{Eh^3}{12(1-\nu^2)}$ the bending stiffness.

The displacement field can be obtained by modal superposition:

$$\tilde{w}_z(x, y) = \frac{1}{M} \sum_n \sum_m \tilde{\Gamma}_{nm}(\omega) \Phi_{nm}(x, y), \quad (41)$$

with the modal magnification factor $\tilde{\Gamma}_{nm}(\omega)$ defined as:

$$\tilde{\Gamma}_{nm}(\omega) = \frac{1}{\omega_{nm}^2 - \omega^2} \left(\tilde{F} \Phi_{nm}(x_F, y_F) + \tilde{R} \Phi_{nm}(x_z, y_z) \right), \quad (42)$$

with \tilde{F} the amplitude of the applied force and \tilde{R} defined as:

$$\tilde{R} = -j\omega c_d \tilde{F} \frac{\sum_n \sum_m \frac{\Phi_{nm}(x_F, y_F) \Phi_{nm}(x_z, y_z)}{\omega_{nm}^2 - \omega^2}}{M + j\omega c_d \sum_n \sum_m \frac{\Phi_{nm}^2(x_z, y_z)}{\omega_{nm}^2 - \omega^2}}. \quad (43)$$

The structural intensity can be derived analytically by substituting the displacement field (41) in the force equations (11),(12),(13) and (14), and subsequently in the intensity equations (9) and (10).

4.2 Contours

Figure 4(a) shows contours of the displacement field at 50 Hz calculated with the WBM with 148 wave functions, and figure 4(b) shows the relative error of the WBM compared to the analytical solution with one million modes. It is clear that the relative error remains within the range of 1%, except where the displacement is close to zero. At those places the error calculation itself is inaccurate due to almost-zero division.

Figure 5(a) shows the intensity field calculated with the WBM with 148 wave functions. It can be seen that energy enters the system at the point force and exits the system at the damper. The intensity is zero at the simply supported edges. Figure 5(b) shows the relative error of the WBM intensity calculation compared to an analytical solution with 400 million modes. Since the convergence of the intensity calculation with modal superposition is slow, a large amount of modes is required [5]. This phenomenon can be seen in table 2. The accuracy of the used ‘‘analytical’’ solution is about 10^{-4} . It can be seen that the error of the WB calculation remains, again, within 1%, except for the places where the intensity is close to zero.

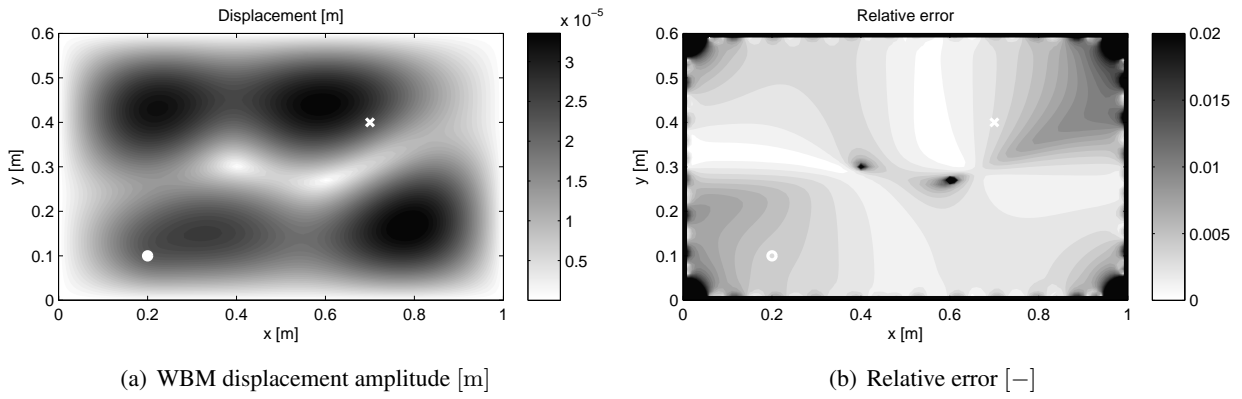


Figure 4: Displacement field calculated with the WBM and relative error at 50 Hz (○ : point force, × : damper).

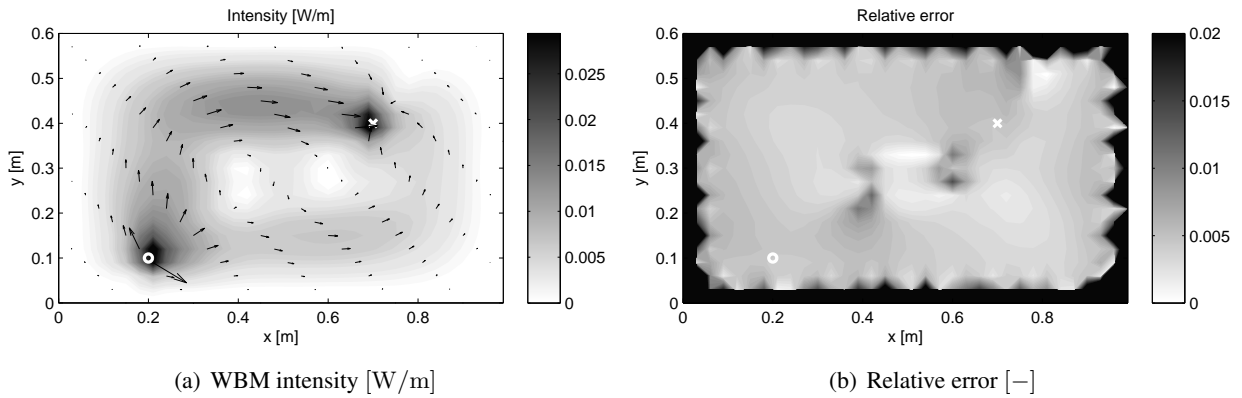


Figure 5: Structural intensity field calculated with the WBM and relative error at 50 Hz (○ : point force, × : damper).

4.3 Convergence

A convergence analysis is performed at two frequencies, at 50 Hz and at 200 Hz. The convergence is verified based on an averaged relative prediction error $\langle \epsilon \rangle$. The averaged prediction error is defined as the average of the relative prediction error in the $n_{rp} = 3$ response points,

$$\langle \epsilon \rangle = \frac{1}{n_{rp}} \sum_{j=1}^{n_{rp}} \epsilon_j, \tag{44}$$

# modes	\bar{w}	ϵ_w	\bar{I}	ϵ_I
1 million	2.8163e-5	6.87e-7	9.1106e-3	6.97e-4
16 million	2.8163e-5	4.14e-8	9.1067e-3	2.00e-4
100 million	2.8163e-5	5.17e-9	9.1059e-3	1.00e-4
400 million	2.8163e-5	Ref	9.1051e-3	Ref

Table 2: Analytical models and their averaged relative error as defined in (44).

with,

$$\epsilon_j = \frac{\left| \sqrt{I_x^2 + I_y^2} - \sqrt{I_{x,\text{ref}}^2 + I_{y,\text{ref}}^2} \right|}{\sqrt{I_{x,\text{ref}}^2 + I_{y,\text{ref}}^2}} \quad (45)$$

The three response points are located at $w_1(0.6\text{m}, 0.42\text{m})$, $w_2(0.24\text{m}, 0.33\text{m})$ and $w_3(0.75\text{m}, 0.12\text{m})$. As reference the analytical solution with 400 million modes is used.

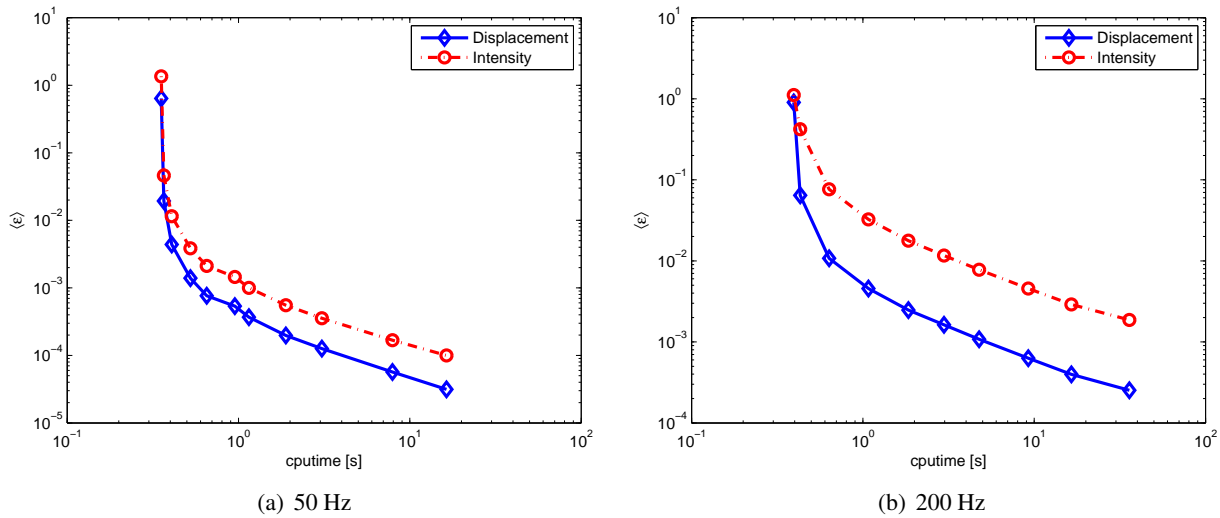


Figure 6: Convergence curves for displacement and intensity calculated with WBM.

Figure 6 plots the averaged relative prediction error $\langle \epsilon \rangle$ on the displacement and the intensity at 50 Hz and at 200 Hz in function of the calculation time. It can be seen that at both frequencies the calculations lead to a quick convergence. The intensity calculation has the same convergence rate as the displacement calculation, but with an offset which is larger at 200 Hz than at 50 Hz, which is a point of further research. Since the WBM shows a better convergence rate than the FEM for displacement calculations [9], and the FEM convergence for intensity calculations suffers from the necessary third-order derivatives, it is expected that the WBM shows a superior convergence for intensity calculation compared to the FEM.

5 Conclusions and future work

This paper proposes a new method for efficient structural intensity calculations in plates based on the WBM. The WBM is a novel deterministic prediction technique, whose superior convergence rate compared to the FEM for displacement calculations has already been shown in previous papers.

The paper starts with the problem description, followed by the description of the WBM for plate bending and the addition of springs and dampers to the system. Subsequently, the extension of the WBM to intensity calculations is explained. The calculation of intensity is a postprocessing step in which the necessary derivatives are determined by deriving the wave functions analytically, which is advantageous for the accuracy.

The last section gives a numerical example, which compares the results obtained with the WBM to results obtained by an analytical solution. In the example, the WBM intensity calculations show a convergence rate similar to the displacement results, which is remarkable for a derived variable.

An interesting next step is the comparison of the WBM intensity calculations with FE calculations. Due to the analytical derivation of the wave functions, which satisfy the governing equations, it is expected that the WBM has a higher convergence rate than the FEM, which has a large loss of accuracy for derived variables. Furthermore, an experimental validation of the obtained numerical results is foreseen [3].

Acknowledgements

Karel Vergote is a Doctoral Fellow of the Fund for Scientific Research - Flanders (F.W.O.), Belgium.

References

- [1] D. Noiseux, *Measurement of power flow in uniform beams and plates*, Journal of the Acoustical Society of America (1970), pp. 238–247.
- [2] J. Verheij, *Cross-spectral density methods for measuring structure-borne power flow on beams and pipes.*, Journal of Sound and Vibration (1980), pp. 133–139.
- [3] J. Arruda, P. Mas, *Localizing energy sources and sinks in plates using power flow maps computed from laser vibrometer measurements*, Shock & Vibration (1998), p. 235.
- [4] O. Zienkiewicz, R. Taylor, *The finite element method - The three volume set (6th ed.)*, Butterworth-Heinemann (2005).
- [5] L. Gavric, G. Pavic, *A finite element method for computation of structural intensity by the normal mode approach*, Journal of Sound and Vibration (1993), pp. 29–43.
- [6] S. Hambric, *Power flow and mechanical intensity calculations in structural finite element analysis*, Journal of Vibration and Acoustics (1990), pp. 542–549.
- [7] R. Lyon, R. DeJong, *Theory and application of statistical energy analysis (2nd ed.)*, Butterworth-Heinemann (1995).
- [8] W. Desmet, *A wave based prediction technique for coupled vibro-acoustic analysis*, Ph.D. thesis, Katholieke Universiteit Leuven, Departement Werktuigkunde, Leuven (1998).
[http://www.mech.kuleuven.be/mod/wbm/phd_dissertations]
- [9] C. Vanmaele, D. Vandepitte, W. Desmet, *An efficient wave based prediction technique for plate bending vibrations*, Computer Methods in Applied Mechanics and Engineering (2007), pp. 3178–3189.
- [10] C. Vanmaele, D. Vandepitte, W. Desmet, *An efficient wave based prediction technique for dynamic plate bending problems with corner stress singularities*, Accepted for publication in Computational Methods in Applied Mechanics and Engineering (2008).
- [11] C. Vanmaele, K. Vergote, D. Vandepitte, W. Desmet, *An efficient wave based prediction technique for the dynamic analysis of 3d plate assemblies*, Submitted for publication in Computational Methods in Applied Mechanics and Engineering (2008).
- [12] E. Trefftz, *Ein gegenstück zum ritzschen verfahren*, in *Proceedings of the Second International Congress on Applied Mechanics*, Zurich, Switzerland (1926), pp. 131–137.
- [13] A. Leissa, *Vibration of plates*, Acoustical Society of America, Woodbury (1993).
- [14] R. Mindlin, *Influence of rotary inertia and shear on flexural motions of isotropic, elastic plates*, Journal of Applied Mechanics ASME (1951), pp. 31–38.
- [15] E. Reissner, *The effect of transverse shear deformation on the bending of elastic plates*, Journal of Applied Mechanics ASME (1945), pp. A69–A77.
- [16] L. Cremer, M. Heckl, E. Ungar, *Structure-borne sound : structural vibrations and sound radiation at audio frequencies*, Springer-Verlag (1973).

-
- [17] C. Vanmaele, *Development of a wave based prediction technique for the efficient analysis of low- and mid-frequency structural vibrations*, Ph.D. thesis, Katholieke Universiteit Leuven, Departement Werktuigkunde, Leuven (2007).
[http://www.mech.kuleuven.be/mod/wbm/phd_dissertations]
- [18] K. Vergote, B. Van Genechten, B. Pluymers, D. Vandepitte, W. Desmet, *A wave based prediction technique for the dynamic response analysis of plates with random point mass distributions*, in *Proceedings of the Ninth International Conference on Computational Structures Technology (CST)*, Athens, Greece (2008).
- [19] M. Junger, D. Feit, *Sound, Structures, and Their Interactions*, Acoustical Society of America (1993).

